

Journal of Optoelectronical Nanostructures



Winter 2025/ Vol. 10, No. 3

Research Paper

Design and Simulation of a High-Performance Electroosmotic Micromixer with Sidewall Obstacles

Elnaz Poorreza¹, Noushin Dadashzadeh^{2*}

¹Departement of Electrical engineering, Aras Branch, Islamic Azad University, Jolfa, Iran

²Department of Electrical Engineering Aras Branch, Islamic Azad University, Jolfa, Iran

Received:

Revised: Accepted: Published:

Keywords:

Electroosmotic,
Electric field,
Microfluidics,
Nanofluidic,
Micromixer

Abstract

Electro-osmotic micromixers represent an active class of micromixers that utilize alternating current (AC) on electrodes. In this work. an electroosmosis-based micromixer has been designed to mix two distinct fluids; an electric potential is imposed across the electrodes with an operating frequency of 8 hertz and maximum value of 0.1 V. To achieve higher efficiency, the sidewalls of the micromixer are fitted with rectangular-shaped barriers. The simulation results based on this structure show that the micromixer achieves an outstanding efficiency of the order of 98%, thereby proving its vast potential in useful applications in a broad spectrum of disciplines in the areas of microfluidics, bioengineering, and biomedical sciences. The influence of manipulating the frequency and potential on the electrodes on the efficacy of mixing has been investigated and the results presented accordingly.

Citation: Noushin Dadashzadeh Assistant Professor, Department of Electrical Engineering Aras Branch, Islamic Azad University, Jolfa, Iran

Iran A High-Performance Electroosmotic Micromixer: How Sidewall Obstacles Influence Design and Simulation. **Journal of Optoelectronical Nanostructures.** 2025; 10 (3): 48-58

*Corresponding author: Noushin Dadashzadeh

Address Department of Electrical Engineering Aras Branch, Islamic Azad University, Jolfa, Iran

. Tell: 00989144925311 Email: noushin.dadashzadeh@iau.ac.ir

1. INTRODUCTION

Over the last few years, microfluidic and nanofluidic systems have emerged as highly potent tools in life sciences and chemistry that initiated immense enhancement in numerous diagnostics as well as therapeutic processes [1-9]. Micromixers are among the most basic building blocks of these systems. They were originally intended to blend samples homogenously as well as efficiently on the scale of the micrometers. Because of the advancements in technology, micromixers of diverse types have been established to meet any kind of application [10]. Because of the advancements in technology, numerous types of micromixers have been designed to meet an extensive spectrum of application areas. The devices are commonly used in numerous different arenas such as medical detection [11-13], biological engineering [14], chemical reactions, material synthesis, cell culture, drug development and screening, biomolecular interactions, and use in environmental protection [10].

Two main categories of micromixers are passive and active [15]. Passive mixing in micromixers takes place by virtue of channel geometry and shape utilizing barriers and split and recombine characteristics of the specific channel designs [16]. Passive micromixers are of interest due to easier fabrication and less energy consumption but can be mixed gradually for high viscosity and low diffusion requirement [12]. On the other hand, active micromixers promote the mixing of fluids by employing external energy from mechanical, thermal, acoustic, magnetic, or electrical. These active mechanisms supply energy into the fluid, generating turbulence, increasing diffusion, and allowing greater control of the mixing rate. Active micromixers are more complex than passive designs. However, they have faster and more precise mixing, which is particularly desirable for applications where reagents or fluids with varying properties need to be mixed rapidly and thoroughly, making them a good choice [17, 18].

Electrokinetic flow is a unique class of electric body force-driven flow or flow subjected to electric body force governed by electric field. Effective micromixing of fluids that generate one of the basic operations in microfluidic devices can facilitate a broad variety of applications ranging from biochemical reaction to medical diagnostics. Electro-osmotic micromixers are active micromixers that draw on an electric field as an external power source. The basic working principle is the interaction between an electric field with low-frequency AC and the inherent charge in the electric double layer (EDL), which creates the electro-osmosis effect. It causes a force in the positively charged

fluid along the channel walls in the electric-field orientation [19].

In this current research work, we conduct a numerical analysis of a micromixer in microfluidics using finite element method. This electroosmosis based ring-type micromixer is designed for mixing of two disparate fluids. In order to achieve maximum efficiency of this mixer device, sinusoidal electric potential is systematically applied between the electrodes with peak value 0.1 V using an operating frequency of 8 hertz. The efficiency of the micromixer is optimized using the semi-circular barrier design of the micromixer. The simulation based on this arrangement demonstrates that the micromixer has an incredibly high mixing efficiency of an impressive 98% earmarking its vast potential to be utilized in highly productive form in an enormous number of disciplines in conjunction with the field of microfluidics, biochemistry, and biomedical sciences. The systematic analysis of the influence of altering the input frequency and potential on the electrodes on the efficiency of the mixing is also undergone and the results are discussed accordingly.

2. GOVERNING EQUATIONS

In an electroosmotic micromixer, the flow field is described by solving Navier-Stokes and continuity equations. Navier-Stokes equations of incompressible flow describe the dynamics of channel flow of fluids as follows [20]:

$$\rho \frac{\partial u}{\partial t} - \nabla \cdot \eta (\nabla \mathbf{u} + (\nabla \mathbf{u})^T) + \rho u \cdot \nabla u + \nabla p = 0$$

$$\nabla \cdot u = 0$$
(1)

The dynamic viscosity is represented by the symbol η and is essentially a measurement of a fluid's internal resistance to flow (SI unit: kg/(m·s)), u shows the velocity of the fluid (SI unit: m/s), ρ denotes the density of the fluid, an important physical parameter measuring the mass of the fluid per unit volume (SI unit: kg/m3), and p denotes the pressure inside the micromixer and measured in units of Pascals (Pa), and this pressure plays an important role in understanding the forces at play in the system. The mixed fluid having undergone the processes appropriate to it in order to be rendered homogeneous in nature is seen to move freely from the specified right end boundary through which it becomes possible to state that total components of stress in a direction normal to the boundary are of vanishing nature and thus point to the absence of any net stress perpendicular to such a boundary, an essential requirement to ensure that the stability and coherence of the fluid dynamics in this boundary be maintained [20]:

$$\mathbf{n} \cdot [-p\mathbf{I} + \eta(\nabla \mathbf{u} + (\nabla \mathbf{u})^T)] = 0$$
(2)

Most solid surfaces carry an electrostatic surface charge when in contact with an electrolyte. Because of the spontaneous surface charge that is present, there is an emergent charged liquid phase on the liquid-solid interface. Electrical double layer is caused by the charge-bearing objects present on the surface in contact with the bounding solution. Electrical double layer is a region of very small thickness located on the fluid-structure interface. The EDL typical thickness is known as Debey length λ_D .

$$\lambda_D = \sqrt{\frac{\varepsilon \varepsilon_0 k_b T}{2 n_i^0 z_i^0 e^2}}$$
(3)

where ε represents solution dielectric constant, ε_0 denotes vacuum permittivity, k_b indicates Boltzmann constant, T shows temperature, n_i is bulk concentration of i_{th} ion, z_i is valence of i_{th} ion, and e is charge at the beginning. Debey length is very small, typically 10 nm, compared to hydraulic diameter of microchannel. Electric potential in thin EDL drops from zeta potential to zero [21].

The resulting electroosmotic flow causes motion of the charged liquid within the restrictions of the electric double layer when an external electric field is imposed. The mechanism subjects the positively charged liquid near the wall surface to an imposed force that results in fluid flow in the direction of the electric field. Viscous transport in this specific direction is facilitated by perpendicular velocity gradients. In the absence of counterforces, the velocity profile reaches the state of near-uniformity over the cross section perpendicular to the wall. This theory replaces the approximation of the thin electric double layer with the use of the Helmholtz-Smoluchowski equation as a representation of an electroosmotic velocity-tangential electric field component correlation [22].

$$u = \frac{\varepsilon_w \zeta_0}{\eta} E_t \tag{4}$$

Here, $\varepsilon_{w} = \varepsilon_{0}\varepsilon_{r}$ denotes the permittivity of the fluid (F/m), ζ_{0} indicates the wall channel zeta potential. E_{t} is the tangent to the surface electric field (E) at the fluid-charged interface. E shows the total electric field vector. n signifies the unit normal vector. The scheme of Fig. 1 presents the effect of electric force field on the fluid flow. Under the influence of an alternating electric voltage inserted between the electrodes, the walls of the channel acquire a negatively fixed surface charge density through the action of the negative zeta potential and due to the process of neutralization that occurs in the EDL. The positive counter ion is seen in the electric double layer as a byproduct of neutralization. Due to

interaction between the positive counter ionic charge within the EDL and the imposed tangential electric field, electroosmotic slip is produced in the direction of the local electric field. Because of the distribution of electrodes that is shown in Figure 2, the electroosmotic flow direction on each side of an electrode is opposite and the direction of electroosmotic flow on the two opposite channel walls is similarly opposite.

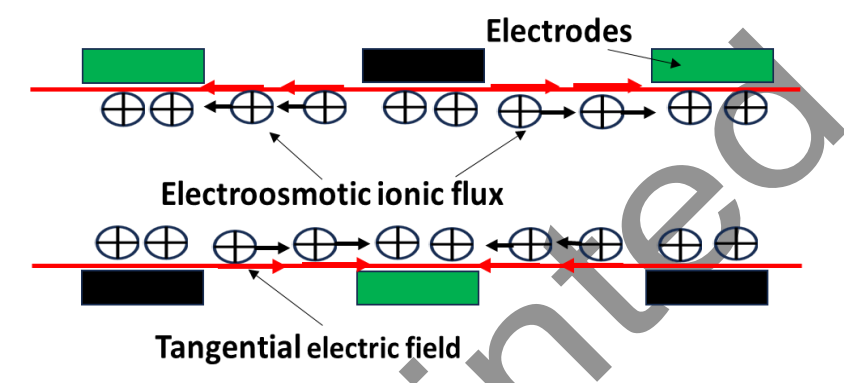


Fig. 1. Schematic of the electric force field on the fluid flow showing formation of electroosmotic phenomenon.

This equation is valid everywhere excluding at the entrance and outlet. With the assumption there are no concentration gradients in the ions carrying the current, it is achievable to represent the current balance in the channel by applying Ohm's law in supplement to the current density balance equation [20]:

$$\nabla \cdot (-\sigma \nabla V) = 0 \tag{5}$$

here σ signifies conductivity (S/m) and the expression within parentheses shows the current density (A/m²)

The potentials that are applied on the electrodes are sinusoidal in time with the same maximum value (V0 = 0.1 V) and the same frequency (8 Hz), but with opposite polarities. The potentials at the electrodes are $\mp V0\sin(2\pi ft)$, where f is the frequency of the signal and t is the time, (see Figure 2). All other boundaries are insulated. The insulation boundary condition prescribes the normal electric field component to be zero.

$$-\sigma \nabla V \cdot \mathbf{n} = 0 \tag{6}$$

At the top half of the inlet (Figure 1), the fluid concentration is c0 and at the bottom half of the inlet, the concentration is zero. Hence, the concentration exhibits a sudden jump from zero to c0 at the center of the inlet boundary.

Mixed solution exits at the right outlet by convective flow and all other boundaries of the proposed micromixer are insulated. Species transport in the system can be expressed by the convection–diffusion equation. In the channel, the convection-diffusion equation for the concentration of the solutes in the fluid was described:

$$\frac{\partial c}{\partial t} + \nabla \cdot (-D\nabla c) = R - u \cdot \nabla c \tag{7}$$

Here c signifies the concentration, D indicates the diffusion coefficient, R represents the reaction rate, and ∇c shows the concentration gradient, and u is the flow velocity. In this specific model, we have assumed R to be zero because the concentration does not get affected by any chemical reaction.

To assess the degree of mixing, or to estimate the efficiency of mixing, the efficiency of mixing, Q, at any cross-section of the microchannel is measured by Equation 8[21]:

$$Q = \left[1 - \frac{\int |c - c_{\infty}| d_A}{\int |c_0 - c_{\infty}| d_A}\right] \times 100\%$$
(8)

where c indicates the concentration of the species along the channel width, c_{∞} signifies in the direction of the concentration of the species in the fully mixed state (i.e. = 0.5), and c_0 shows the concentration of the species in the fully unmixed state or pure condition (i.e. $c_0 = 0$ or 1)

3. MODEL GEOMETRY

A schematic of the proposed micromixer was shown in Figure 2(a). A sinusoidal electric potential of 0.1 V with frequency 8 Hz was utilized. The justification of choosing the frequency of 8 Hz, is due to the recent study [23]. On the whole, the mixing enhances with the increase in the field parameters such as frequency and applied voltage. The impact of the frequency in changing the field influences the outcome. Efficiency in mixing is based on the actuation frequency in the case of using an alternating field. This is because the reality that in flows of low Reynolds numbers there is no possibility of chaotic mixing because of the absence of turbulence but the electric frequency is able to toggle the flow between stable and unstable zones creating a mixing force. In order to simulate the conceptualized micromixer and perform numerical implementation, COMSOL Multiphysics 5.4 was used. The three physics of Laminar Flow, Electric currents, and diluted-species transport were coupled in order to perform the simulation. Fig. 2(b) shows the physics and boundary conditions of the micromixer.

The fluid properties are enumerated in Table 1.

Table 1. Values of the designed micromixer [24, 25]

Parameter	Value	Explanation
ρ	1000 Kg/m^3	Density of fluid
η	10 ⁻³ Pa.s	Viscosity of the fluid
U_0	0.1 mm/s	Velocity of the inlet
ε_r	80.2	Relative permittivity of the fluid
ζ	-0.1 V	Zeta potential
σ	0.118[S/m]	Conductivity value of the ionic solution
D	10 ⁻¹¹ m ² /s	Diffusion coefficient
C_0	1 mol/ m ³	Initial concentration of the fluid

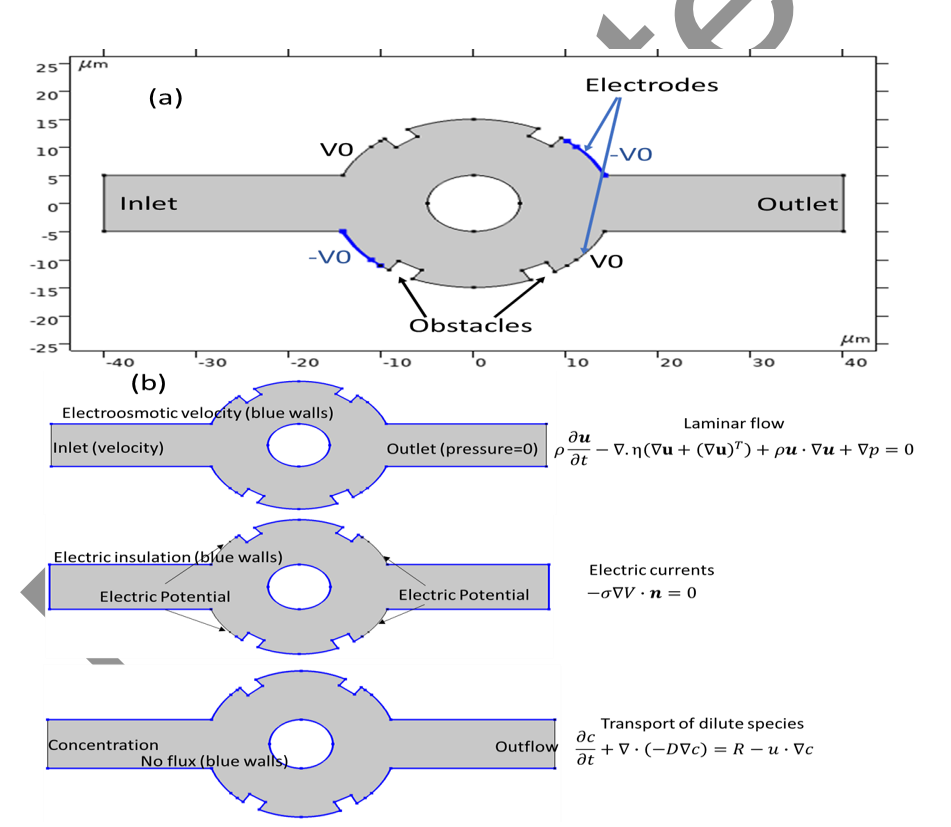


Fig. 2. (a) Schematic view of the proposed micromixer with symmetric electrodes on the wall of the mixing chamber and four rectangular-shaped

obstacles embedded on the walls of the micromixer (b) physics and boundary conditions of the micromixer

4. RESULTS AND DISSCUSSION

4.1. Simulation of the electric field profile, concentration and mixer efficiency

Figure 4 shows streamline inside the micromixer at three-time steps: (a), t = 0.28 s, and (b), t = 0.34 s, when the alternating electric field is at peak magnitude. This particular demonstration elucidates the phenomenon of electroosmotic recirculation in the fluid medium, which causes a deep agitation on the flow dynamics, and this agitation is manifested mostly in the form of rotating vortices that are strategically positioned in close proximity to the electrodes. Furthermore, it clarifies the fact that the electroosmotic recirculation of the fluid efficiently imposes the intense agitation of the flow, which is normally depicted as rotating vortices that are located near the electrodes. The basic mechanisms that are at the core of attaining operational mixing involve a complicated interaction involving the repetitive stretching and folding of fluid elements, which is coupled with diffusion processes that occur at small scales.

For the proposed micromixer, an external voltage is applied in a systematic manner to generate electric fields, which induce fluid motion or aid in the process of mixing by several mechanisms. Figures 5(a) and 5(b) are the graphical representation of electric potential $(\pm V0)$ and the resulting electric field for the electroosmotic micromixer, respectively. As can be mentioned and are evident from simulations, the maximum values for both electric potential and electric field distribution are in close proximity to the electrodes, and therefore the significance of their spatial arrangement in the overall performance of the micromixer.

Figure 6(a, b, c, d, e, f) show the concentration levels achieved at a steady state. By introducing the AC electric field, an improved mixing is can be seen, which is attributable to the alternating vortices characteristically implanted within the flow dynamics. From the complete graphical depiction provided, one may safely accomplish with a reasonable degree of certainty that the concentration levels obtained at the output have fluctuations that are directly relative to the frequency of the applied electric field.

Figure 7 is used to demonstrate the species concentration outlines at the outlet of the microchannel at some specific points in time, which are properly recognized in the figure legend for clarity and reference. Figure 8 gives a

detailed clarification of the efficiency of mixing across the entire cross-sectional width of the channel, which has been thoroughly assessed at a number of different time points that are likewise spelled out in the figure legend, thereby giving a comprehensive overview of the complicated mixing dynamics that occur within the microchannel at various times of the mixing process. It is worthwhile to observe here that, due to the inherently random nature of the perturbation given to the system, the mixing efficiency profile adheres to a highly non-uniform trend that can be observed across the various instances considered. All of these results go to corroborate the statement that a high level of mixing efficiency can be obtained by using the proposed mixer, as has been established in this comprehensive study. On the basis of Equation (8) as a basis for computation, the efficiency of mixing the fluids is found to reach a high level of nearly 98%, thereby showing the success of the proposed model. Table 2 shows the micromixer's performance against previously published electrokinetic micromixers based on key metrics.

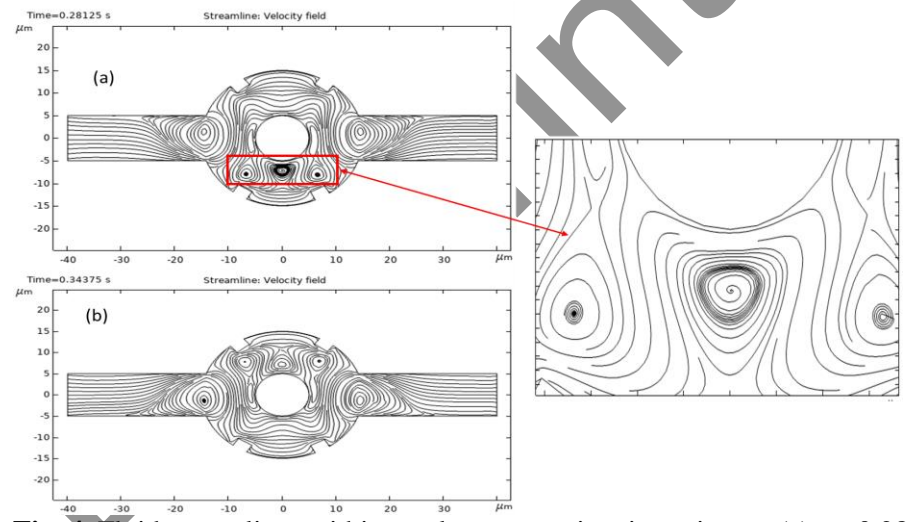


Fig. 4. Fluid streamlines within an electroosmotic micromixer at (a) t = 0.28 s, and (b), t = 0.34 s, when the AC electric field is applied.

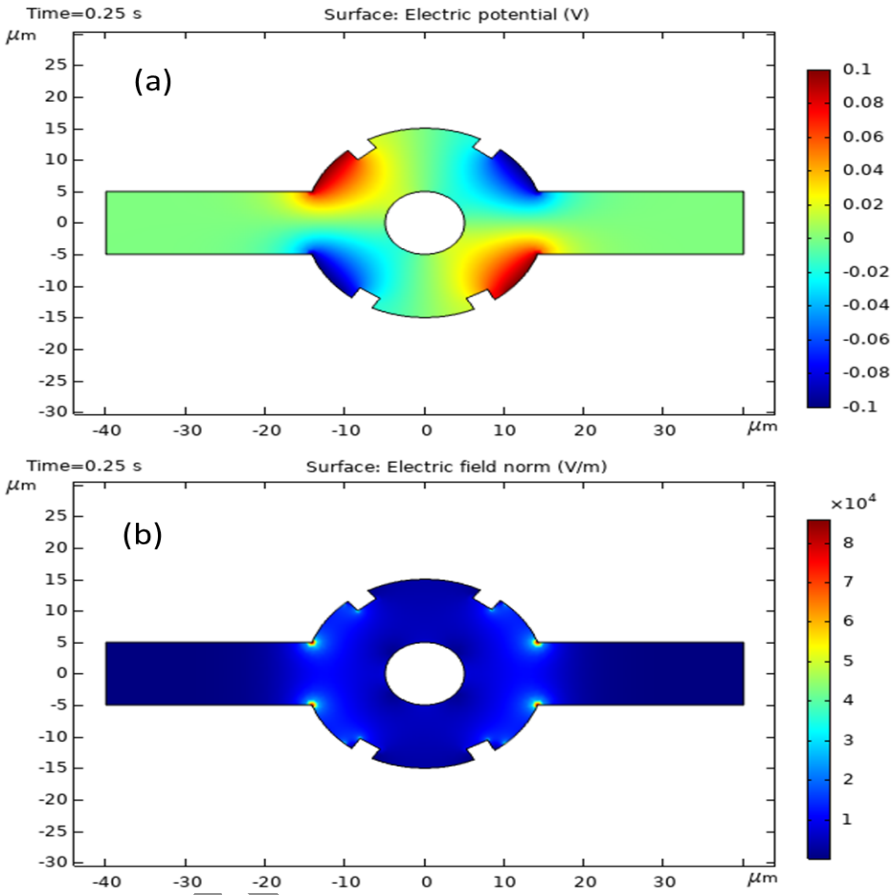


Fig. 5. (a) Simulation of electric potential $(\pm V0)$ for the electroosmotic micromixer (b) alongside electric field at t=0.25 s.

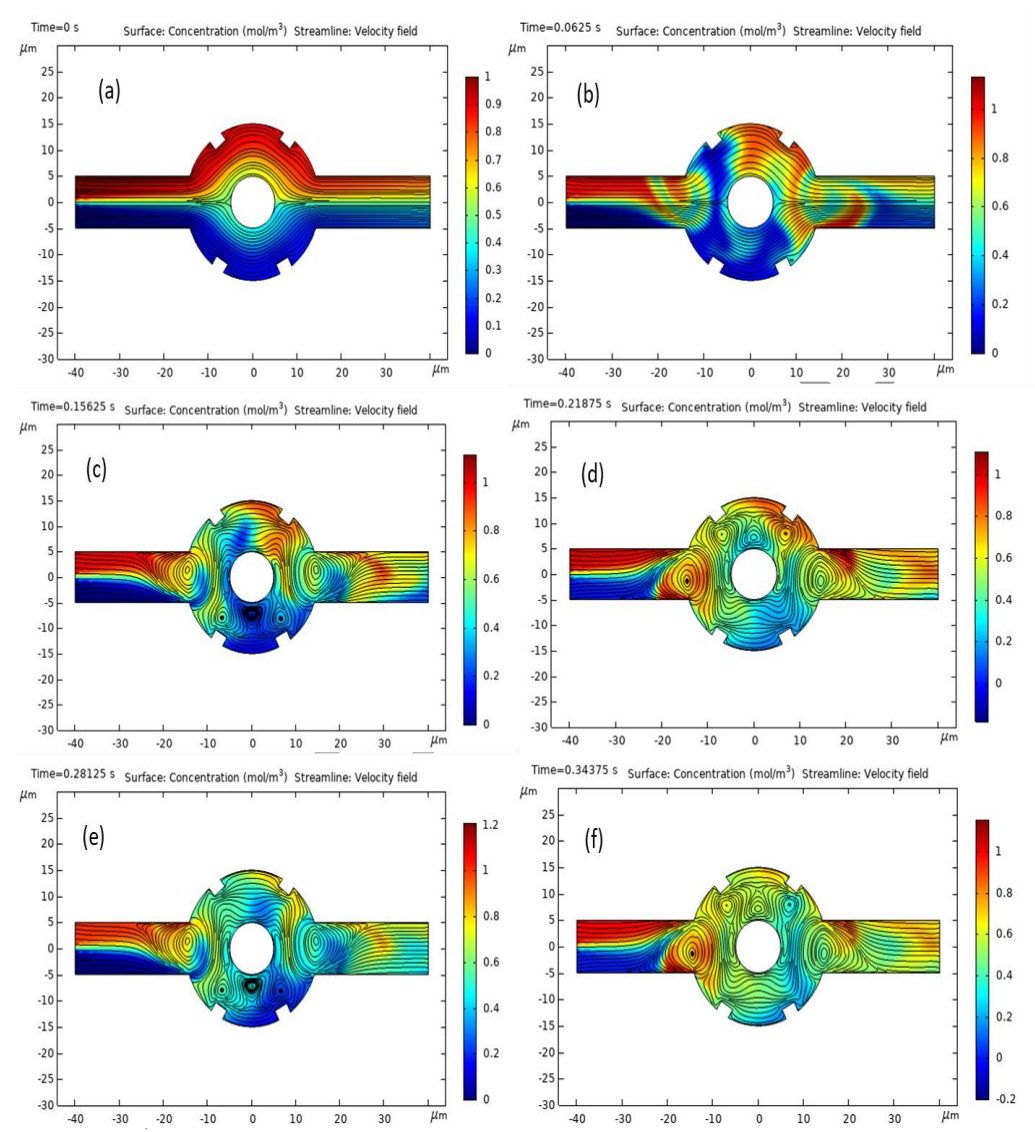


Fig. 6. Concentration plot of the micromixer: (a) time = 0 s, (representing the steady-state solution devoid of an electric field) (b), time = 0.06 (c) time: 0.15 s, (d) time: 0.21 s, (e) time: 0.28 s, and (f) time: 0.34 s.

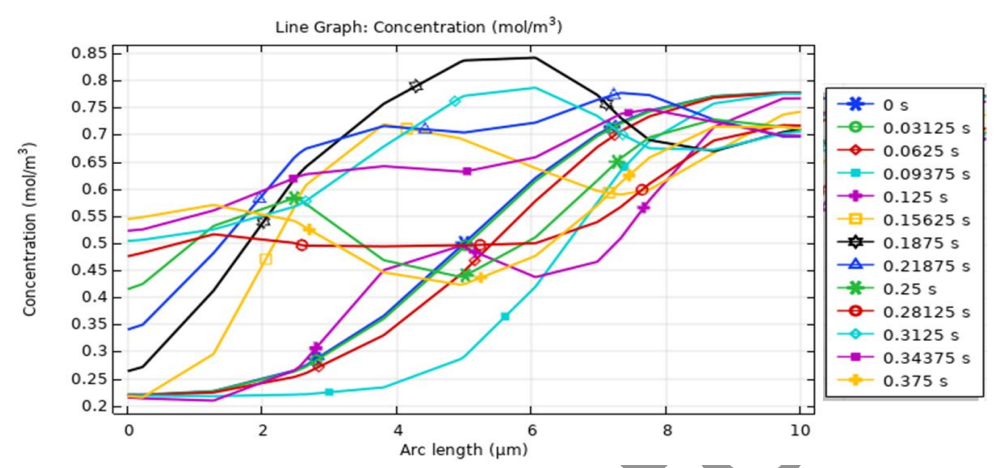


Fig. 7. Concentration profiles of species at the outlet of the microchannel at various temporal instances (as denoted in the figure legend).

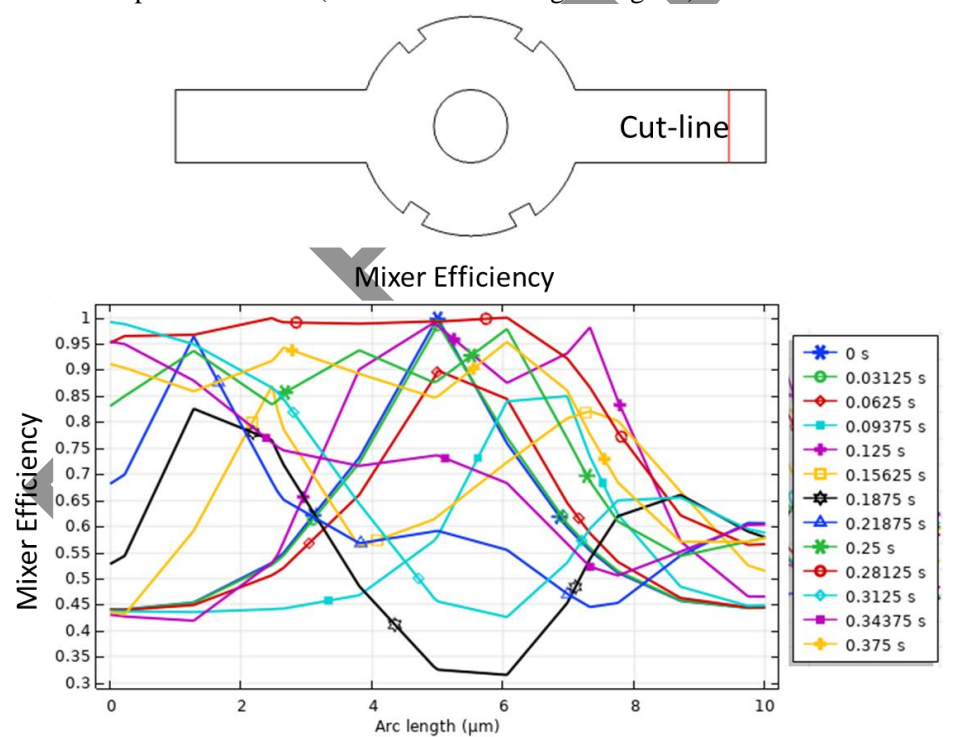


Fig. 8. Simulation of mixing efficiency across the channel's cross-section at distinct times.

Table 2. our proposed micromixer's performance against previously published electrokinetic micromixers based on key metrics

Mixer Type & Ref.	Mixing Efficiency	Operating Conditions (V, f)	Key Advantage	Key Limitation
This Work	>98%	0.1 V, 8 Hz	Ultra-low voltage, simple fabrication	Performance optimized for specific (V, f)
Electroosmotic micromixer [21]	>90%	5 V, 8 Hz	Si ₃ N ₄ insulating layer on electrodes	High voltage, Joule heating
induced-charge electrokinetic [25]	~94%	N/A	Rapid mixing	Complex multi- phase electronics
Electroosmotic micromixer [10]	~99%	1-3 V, 8 Hz	Good efficiency	Complex electronics

4.2. The impact of variation of frequency on mixer efficiency

At very low frequencies the flow can become so steady that chaotic advection is diminished. At the high frequency ranges, the electric field changes fast and ions might not get enough time to fully respond. Figure 9 illustrates the mixer efficiency in the with and without the presence of obstacles cases through the modification of the frequency used. From what can be seen, in both cases, in the frequency range of 4 Hz the efficiency is low and by raising the frequency to 6 and 8 Hz it has a near 98% value. Raising the frequency any further reduces the mixer efficiency.

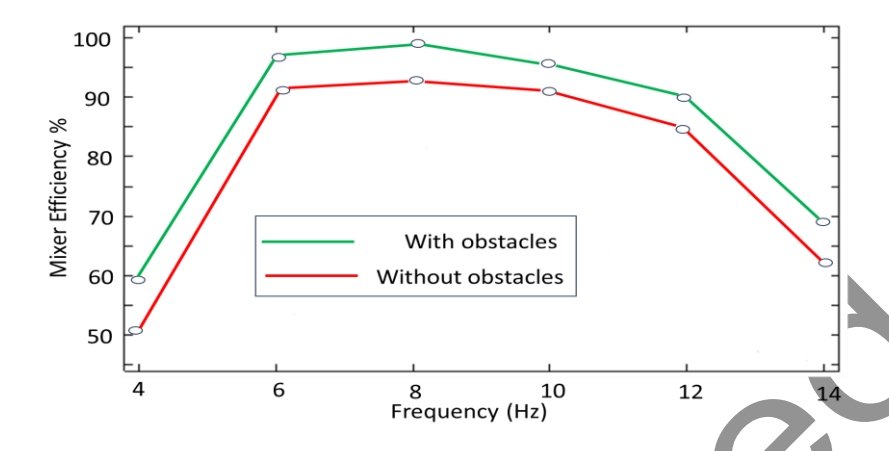


Fig. 9. Profile of the influence of changing the applied frequency on mixer efficiency.

4.3. The influence of variation of potential on mixer efficiency

Increasing the voltage in electrokinetic devices can affect mixing efficiency but depends on the device design and on the particular mechanism of mixing. But in simple laminar electroosmotic flow, raising the voltage alone is not likely to significantly improve the mixing unless accompanied by other measures (e.g., obstacles, asymmetrical geometries). As shown in Fig. 10, in both cases of with obstacles and without obstacles, when the voltage is below 0.1 V, the mixing efficiency of mixer increases with increasing the electric potential on the electrodes. While, for voltages above 0.1 V, a maximum mixing efficiency (98%) can be achieved.

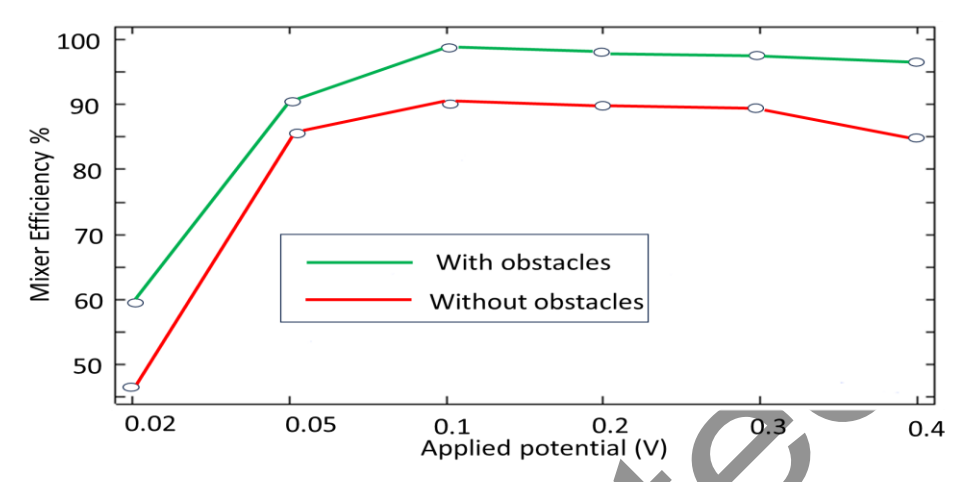


Fig. 10. Profile of the influence of changing the applied potential on mixer efficiency.

5. CONCLUSION

Micromixers can be reflected as one of the most important devices in micromachines and have played a vital role in a different array of applications that encompass, but are not limited to, biomedical diagnosis, chemical analysis, drug delivery, and etc. The phenomenon of electroosmotic flow as an active mixing, has attracted more attention in developing the perfect mixing performance of microfluidic systems. In this study, a micromixer that operates based on the electroosmosis has been designed to mix two different fluids; a sinusoidal electric potential is imposed across the electrodes, by a peak value of 0.1 V and a systematic operating frequency of 8 hertz. In an effort to further enhance the operational efficiency of the micromixer, rectangular-shaped obstacles have been incorporated along the sidewalls of the micromixer. Based on the structural configuration established in this research, the simulation results show that the micromixer attains an efficiency approximately 98%, thereby underscoring its substantial potential for the applications across a diverse spectrum of disciplines, particularly the fields of microfluidics and biomedical sciences.

REFERENCES

[1] Y. Gong and X. Cheng, Numerical investigation of electroosmotic mixing in a contraction—expansion microchannel, *Chemical Engineering*

- *and Processing-Process Intensification*, 192, (2023) 109492. https://doi.org/10.1016/j.cep.2023.109492
- [2] R. Derakhshan, A. Mahboubidoust, and A. Ramiar, Design of a novel optimized microfluidic channel for CTCs separation utilizing a combination of TSAWs and DEP methods, *Chemical Engineering and Processing-Process Intensification*, 167, (2021) 108544. http://dx.doi.org/10.1016/j.cep.2021.108544
- [3] D. Wang *et al.*, A Novel Microfluidic Strategy for Efficient Exosome Separation via Thermally Oxidized Non-Uniform Deterministic Lateral Displacement (DLD) Arrays and Dielectrophoresis (DEP) Synergy, *Biosensors*, 14 (4) (2024) 174. https://doi.org/10.3390/bios14040174
- [4] T. N. Adams, A. Y. Jiang, P. D. Vyas, and L. A. Flanagan, Separation of neural stem cells by whole cell membrane capacitance using dielectrophoresis, *Methods*, 133, (2018) 91-103. https://doi.org/10.1016/j.ymeth.2017.08.016
- [5] N. Dadashzadeh, Effect of dielectric constant on the plasma characteristics of a dielectric barrier discharge reactor, Journal of Optoelectronical Nanostructures, 35(4) (2024) 53 10.30495/JOPN.2024.33727.1329
- T. Dehghani, F. S. Moghanlou, M. Vajdi, M. S. Asl, M. Shokouhimehr, and M. Mohammadi, Mixing enhancement through a micromixer using topology optimization, *Chemical Engineering Research and Design*, 161 18.(۲۰۲۰), ^{NA 7}-V http://dx.doi.org/10.1016/j.cherd.2020.07.008
- [7] A. Shahidian and S. Tahouneh, A comprehensive overview of micromixers and micropumps in biomechanical applications, *Journal of Computational & Applied Research in Mechanical Engineering* (*JCARME*), (2025). https://doi.org/10.22061/jcarme.2025.10035.2349
- [8] K. Karthikeyan and L. Sujatha ,Study of permissible flow rate and mixing efficiency of the micromixer devices," *International Journal of Chemical Reactor Engineering*, 17(1)(2019), 20180047. http://dx.doi.org/10.1515/ijcre-2018-0047
- [9] P. Gupta and S. S. Bahga, Mechanism of sinuous and varicose modes in electrokinetic instability, *Physical Review E*, 110 (3) (2024) 035106. http://dx.doi.org/10.1103/PhysRevE.110.035106
- [10] A. Khoshnod, R. Shahsavandi, and K. Hosseinzadeh, Investigation of mixing performance in electro-osmotic micromixers through rigid baffle design and parameter optimization, *Scientific Reports*, 15 (1) (2025) 1-31. https://doi.org/10.1038/s41598-025-01812-7
- [11] A. A. Sayad *et al.*, A microfluidic lab-on-a-disc integrated loop mediated isothermal amplification for foodborne pathogen detection,

16

- *Sensors and Actuators B: Chemical*, 227, (2016) 600-609. http://dx.doi.org/10.1016/j.snb.2015.10.116
- [12] S. F. Javed, M. E. Khan, Z. Yahya, M. J. Idrisi, and W. Tenna, Performance analysis of three-dimensional passive micromixers using k-means priority clustering with AHP-based sustainable design optimization, *Scientific Reports*, 15 (1) (5.54) 1-17 https://doi.org/10.1038/s41598-025-03183-5
- [13] A. Kumar, N. K. Manna, S. Sarkar, and N. Biswas, Enhancing mixing efficiency of a circular electroosmotic micromixer with cross-reciprocal electrodes, *Physics of Fluids*, 36 (8) (2024). http://dx.doi.org/10.1063/5.0225659
- [14] A. J. Conde, I. Keraite, A. E. Ongaro, and M. Kersaudy-Kerhoas, Versatile hybrid acoustic micromixer with demonstration of circulating cell-free DNA extraction from sub-ml plasma samples, *Lab on a Chip*, 20 (4) (2020) 741-748. http://dx.doi.org/10.1039/C9LC01130G
- [15] S. R. Bazaz, A. Sayyah, A. H. Hazeri, R. Salomon, A. A. Mehrizi, and M. E. Warkiani, Micromixer research trend of active and passive designs, *Chemical Engineering Science*, (2024) 120028. http://dx.doi.org/10.1016/j.ces.2024.120028
- [16] M. Waqas, A. Palevicius, V. Jurenas, K. Pilkauskas, and G. Janusas, Design and Investigation of a Passive-Type Microfluidics Micromixer Integrated with an Archimedes Screw for Enhanced Mixing Performance, *Micromachines*, 16 (1) (2025) 82. http://dx.doi.org/10.3390/mi16010082
- [17] A. Najafpour, S. Akbari, K. Hosseinzadeh, M. A. Bijarchi, A. Ranjbar, and D. Ganji, Active 3D electro-osmotic control micromixers: Effects of geometry, DC, and AC electric fields on mixing performance, *International Communications in Heat and Mass Transfer*, 165 (2025) 109033.http://dx.doi.org/10.1016/j.icheatmasstransfer.2025.109033
- [18] E. Poorreza, Computer-Assisted Modeling and Simulation of a Dielectrophoresis-based Microseparator for Blood Cells Separation Applications, *Chromatographia*, (2025) 1-18. https://doi.org/10.1007/s10337-025-04385-9
- [19] M. Wu, Y. Gao, A. Ghaznavi, W. Zhao, and J. Xu, AC electroosmosis micromixing on a lab-on-a-foil electric microfluidic device, *Sensors and Actuators B: Chemical*, 359, (2022) 131611. http://dx.doi.org/10.1016/j.snb.2022.131611
- [20] A. Agarwal, A. Salahuddin, H. Wang, and M. J. Ahamed, Design and development of an efficient fluid mixing for 3D printed lab-on-a-chip,

- *Microsystem Technologies*, 26 (8) (2020) 2465-2477. https://doi.org/10.1007/s00542-020-04787-9
- [21] R. H. Vafaie, M. Mehdipoor, A. Pourmand, E. Poorreza, and H. B. Ghavifekr, An electroosmotically-driven micromixer modified for high miniaturized microchannels using surface micromachining, *Biotechnology and Bioprocess Engineering*, 18 (**\forall^*) 594-605 https://doi.org/10.1007/s12257-012-0431-5.
- [22] X. Niu and Y.-K. Lee, Efficient spatial-temporal chaotic mixing in microchannels, *Journal of Micromechanics and microengineering*, 13 (3) (2003) 454. http://dx.doi.org/10.1088/0960-1317/13/3/316
- [23] H. Chen, Y. Zhang, I. Mezic, C. Meinhart, and L. Petzold, Numerical simulation of an electroosmotic micromixer, in *ASME International Mechanical Engineering Congress and Exposition*, 37165 (2003) 653-658.
- [24] N. J. Ghahfarokhi, M. Bayareh, A. A. Nadooshan, and S. Azadi, Mixing enhancement in electroosmotic micromixers, *Journal of Thermal Engineering*, 7 (2) (2021) 47-57. http://dx.doi.org/10.18186/thermal.867134
- [25] M. Nazari, P.-Y. A. Chuang, J. A. Esfahani, and S. Rashidi, A comprehensive geometrical study on an induced-charge electrokinetic micromixer equipped with electrically conductive plates, *International Journal of Heat and Mass Transfer*, 146 (2020) 118892 http://dx.doi.org/10.1016/j.ijheatmasstransfer.2019.118892.